Title

Surface modification of flax nonwovens for the development of sustainable, high performance, and durable calcium aluminate cement composites

Authors

Gonzalez-Lopez, Laura
Claramunt, Josep
Hsieh, You-Lo
et al.

Publication Date

2020-06-01

DOI

10.1016/j.compositesb.2020.107955

Peer reviewed

Composites Part B 191 (2020) 107955

Contents lists available at ScienceDirect

Composites Part B

journal homepage: www.elsevier.com/locate/compositesb

Surface modification of flax nonwovens for the development of sustainable, high performance, and durable calcium aluminate cement composites

Laura Gonzalez-Lopez [a], Josep Claramunt [b], You-Lo Hsieh [c], Heura Ventura [a], Mònica Ardanuy [a,*]

[a] Departament de Ciència i Enginyeria de Materials, Universitat Politècnica de Catalunya, Colom 1, 08222, Terrassa, Spain
[b] Departament d'Enginyeria Agroalimentària i Biotecnologia, Universitat Politècnica de Catalunya, Av. del Canal Olímpic 15, 08860, Castelldefels, Spain
[c] Fiber and Polymer Science, University of California, Davis, CA, 95616, United States

ARTICLE INFO

Keywords:
Fiber reinforcement
Calcium aluminate cement
Composite
Aging
Mechanical properties

ABSTRACT

The aim of this paper is to evaluate the influence of sustainable surface treatments —performed on flax nonwoven fabrics as textile reinforcement— on the durability of calcium aluminate cement (CAC) based composites. Two treatments are considered: an alkaline treatment (for increased stability and adhesion), and a treatment with soybean oil (to reduce fiber degradation). The cement hydration was studied by analysis of back-scattered scanning electron microscopy images, which revealed variations nearby the fibers owing their capacity for water absorption and presence of oil on the surface. A retarding effect on cement hydration was observed on the composites prepared with the oil-treated fabrics. The composites containing the alkali treated fabrics had better mechanical properties and also the highest durability. For these composites it was found an optimized fiber-matrix adhesion and penetrability of the cement to the fabric.

1. Introduction

Recently, the building industry has increased attention on natural fiber cement-based biocomposites as lightweight materials with good mechanical performance and low environmental impact. Lots of interesting works have been published describing the mechanical performance of these biocomposites reinforced with a wide variety of randomly dispersed lignocellulosic fibers such as sisal, flax, jute, fique or hemp, among others. Other few studies describe the performance of composites with these natural fibers in the form of textile structures [1,2]. These textile reinforcements lead to new sustainable construction materials with high strength under flexural and tensile forces that can be used in a wide range of applications, such as façade panels [3], reinforcement and repair systems for masonry strengthening [4,5], and thin mortar panels [6–8], among others.

However, one of the main drawbacks of the natural fibers for applications in cement composites is their high level of moisture absorption–desorption, owing to the dimensional variation produced when the changes in this environmental moisture diffuse through the matrix, leading to materials with low durability to accelerated wet/dry cycling. Therefore, in order to increase durability in natural fiber reinforced cement composites, the reduction of the moisture absorption of the fibers is a key factor. To that purpose, a possible treatment is the removal of non-cellulosic components [9–12]. Other way to reduce in a higher degree this moisture absorption while protecting the fibers from the hydrophilic matrix at the same time, is to make their surface more hydrophobic.

Nowadays, most hydrophobic surface modification of fibers incorporate reagents, such as fluorocarbons, silicones and alkylsiloxanes. Their cost, sustainability and environmental concerns limit the applications of these processes and chemicals in cellulose cement composite materials. However, vegetable oils are an excellent green alternative as proposed by Dankovich and Hsieh [13].

On the other hand, another problem linked with the low durability to wet/dry cycles of natural fiber cementitious composites is the presence of calcium hydroxide (Portlandite) in the hydrated Portland cement matrix, which degrades de fibers [14,15]. Many papers describe the use of pozzolanic additions [5,8,16,17] or the carbonation process [18–21] for reducing or removing the Portlandite content in the hydrated cement. Although leading to some improvements, these strategies are not enough to guaranty the long-term durability of the material. Less studied is the use of other cement-based matrices free of Portlandite, like calcium aluminate cements.

Calcium aluminate cements (CAC) were developed as an alternative

* Corresponding author.
E-mail addresses: laura.gonzalez.lopez@upc.edu (L. Gonzalez-Lopez), josep.claramunt@upc.edu (J. Claramunt), ylhsieh@ucdavis.edu (Y.-L. Hsieh), heura.ventura@upc.edu (H. Ventura), monica.ardanuy@upc.edu (M. Ardanuy).

https://doi.org/10.1016/j.compositesb.2020.107955
Received 8 March 2019; Received in revised form 12 February 2020; Accepted 4 March 2020
Available online 5 March 2020
1359-8368/

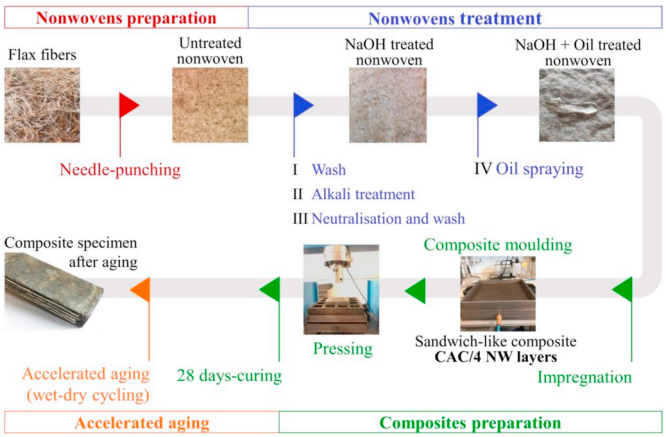

Fig. 1. Scheme of the samples production and treatment, from the formation of the nonwoven fabric and the different treatments applied, to the preparation of the composites and the accelerated aging.

to Portland cement for their better properties in sulfate ambient. In these cements, the monocalcium aluminate (CA) is the major phase, and the hydration products formed depend on the curing temperature and water content. At ambient temperature, the hexagonal calcium aluminates CAH_{10} ($CaAl_2[OH]_8[H_2O]_{5.4}$) are formed, which can transform—at higher temperatures and water content—into the thermodynamically stable form C_3AH_6 ($Ca_3Al_2(OH)_{12}$) [22,23]. These forms, together with the aluminum hydroxide, are the main products of the chemical reactions. The absence of Portlandite make this cement suitable for more durable cellulosic fiber–cement composites. Nonetheless, the conversion of metastable phases into stable ones leads to an increase on the porosity and, hence, to a decrease on the mechanical properties. This effect can be considerably reduced whether a water/cement (w/c) ratio under 0.4 is used [24]. This fact has been taken into account by many building standards that determine the limitations in the use of such a kind of cement for structural purposes.

In this work, the influence of sustainable surface treatments of flax nonwoven reinforcement on the durability of calcium aluminate based cement composites is experimentally evaluated. To this purpose, needle-punched nonwoven fabrics—specifically designed for cement-based matrix reinforcement—have been subjected to surface treatments in order to remove non-cellulosic components, and to make them hydrophobic. The removal of the non-cellulosic components was achieved by means of a chemical treatment with NaOH. Soybean oil applied through a one-step spraying method on the fabrics was performed to make the fabrics hydrophobic. The effect of these surface treatments on the microstructure, mechanical performance and durability of calcium aluminate cement-based composites was then assessed through the analysis of SEM and BSEM images, EDS analysis, and their flexural performance before and after a wet-dry cycling (accelerated aging) process.

2. Materials and methods

Flax fibers with an average length of 6 cm, provided by *Fibers Reserche Development* of the *Technopole de l'Aube*, Champagne (France) were used to prepare the nonwoven reinforcement. The composition of these fibers, according to the provider, was of 77.1 ± 0.0% cellulose, 6.7 ± 0.2% hemicelluloses, 2.6 ± 0.2% lignin, 13.1 ± 0.3% solubles (gums, fatty acids, esters of fatty acids, waxes or other unsaponificable resins) and 0.5 ± 0.0% minerals.

Calcium aluminate cement (CAC) "Electroland"—supplied by *Cements Molins*, Barcelona (Spain)—was used as matrix. Its main chemical composition in oxide equivalent (wt.%) is Al_2O_3 (41.5%), CaO (38%), Fe_2O_3 (10.5%), FeO (4.5%), SiO_2 (3%). The main mineralogical phase is $CaAl_2O_4$, followed by Ca_2FeAlO_5. Other minority components are: $Ca_{12}Al_{14}O_{33}$, ß-Ca_2SiO_4, $Ca_3TiFe_2O_8$ and FeO.

Fig. 1 shows the scheme of the procedure followed for the nonwovens production and treatment, and for the composites preparation and aging. It consisted of four steps: a) nonwovens preparation, b) nonwovens treatment —which are further detailed in section 2.1—, c) composites preparation, and d) accelerated aging if the samples —which are further described in section 2.2—.

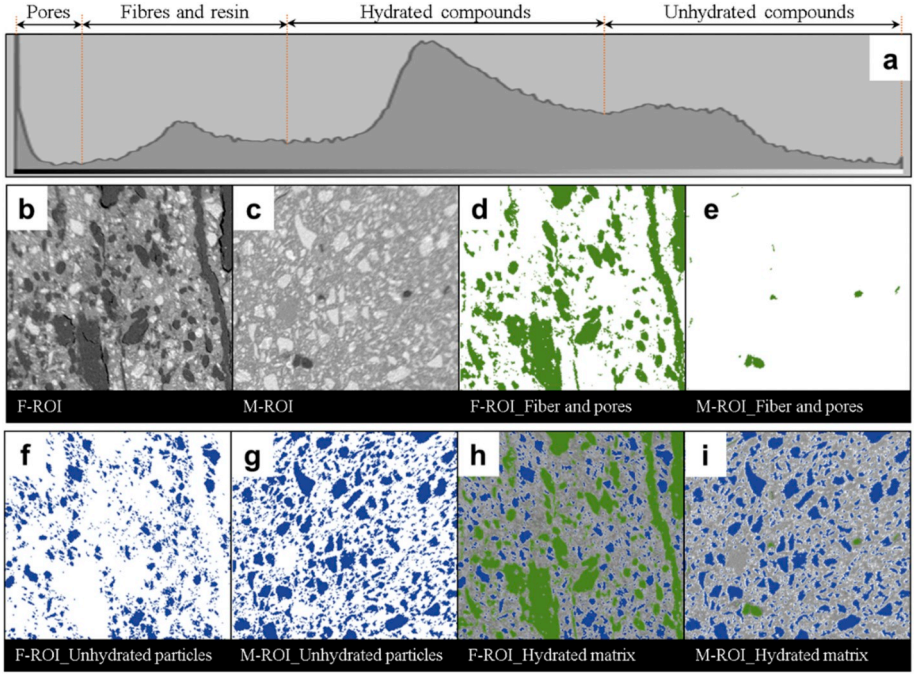

Fig. 2. Procedure of image treatment to determine the hydration degree. **(a)** Grey spectrum for threshold calibration. Images of the regions of interest (ROI) corresponding to the fibers **(b)** and the matrix **(c)**. Pore and fiber detection in the fiber ROI **(d)** and in the matrix ROI **(e)**. **(f, g)** Anhydride areas detection. **(h, i)** After the image treatment, the hydrated areas are differentiated in grey.

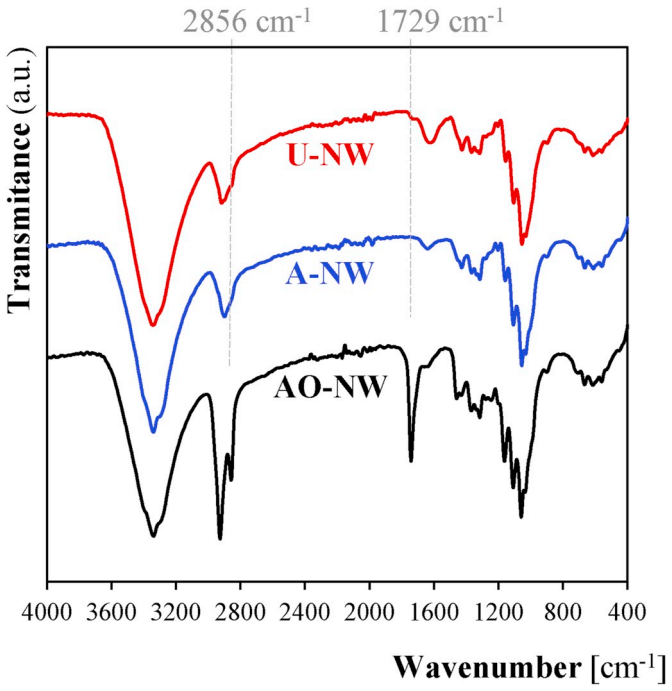

Fig. 3. FTIR spectra of untreated (U-NW), NaOH treated (A-NW) and NaOH then soybean oil treated (AO-NW) nonwovens.

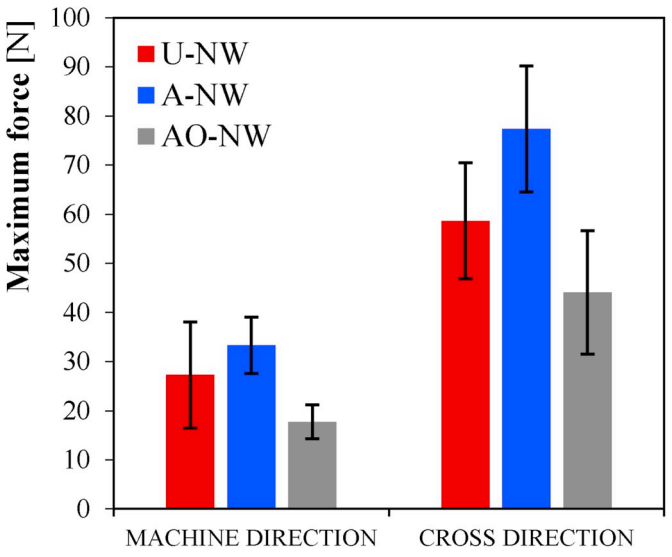

Fig. 4. Values of maximum force in machine and cross directions for the untreated (U-NW), NaOH treated (A-NW) and NaOH then soybean oil treated (AO-NW) nonwovens.

2.1. Preparation, surface treatments and characterization of flax nonwoven

Flax nonwovens were prepared on a DILO OUG–II–6 double needle-punching machine (*Dilo Group*, Germany) following the methodology presented in previous works [3,25]. Briefly, flax fibers were first opened and carded to form thin webs, which were cross-layered to form batts of multiple layers. Then, the batts were entangled with a needle stroke of 750 rpm to form needle-punched nonwoven in 2.5 mm thickness and 400 g/m^2 areal weight.

Two surface treatments were performed on the nonwovens, using untreated nonwovens (U-NW) for comparison. The first treatment was to remove the non-cellulosic components (A-NW) by washing with 5% non-ionic detergent Sandozin and rinse at 60 °C with water followed by washing and rising with water at room temperature to remove dirt and aqueous soluble substances. Afterwards, the nonwovens were subjected to 5% NaOH at a 1:50 liquor ratio at boil for 30 min, followed by neutralization with 1% acetic acid in water and oven-drying at 60 °C for 24 h.

The second treatment (AO-NW) involves covering A-NW with soybean oil by spray-coating process [13] in which 1 w/w% soybean oil/-acetone was sprayed at a fixed 30 cm distance using a spray gun and dried at 60 °C for 24 h. A total of 100 g solution was sprayed, consecutively, onto both sides of each 40 × 40 cm^2 nonwoven fabric, with a time of application around 1 min to allow a homogeneous coating. This spray coating process minimizes the use of chemical reagents [26,27].

All nonwovens were conditioned at 20 ± 2 °C and 65 ± 2% for a minimum of 24 h prior to testing.

Moisture regain values on the fabrics were determined following the DIN 54351 standard, and the water absorption was determined by dropping a 0.5 mL water drop on the surface and measuring the time for the drop to penetrate through the fabric.

To determine the breaking force of the nonwovens, tensile tests based on the UNE-EN ISO 13934-1 Standard were performed in a MTS dynamometer (*MTS Systems*, USA) with a 5 kN load cell at a 100 mm/min displacement rate.

Changes on the chemical compositions were determined using Fourier transformed infrared spectroscopy (FTIR). FTIR spectra were collected on a FTIR Nicolet 6700 spectrometer (*Thermo Scientific*, USA), using an ATR adapter provided with a diamond disc. Each spectrum was obtained from an accumulation of 32 scans with a wavelength resolution of 4 cm^{-1}, and 6 spectra per sample were taken.

2.2. Production and characterization of cement composites

Three kind of composite laminates were prepared for this study: with untreated reinforcement (CAC/U-NW), with alkaline-treated reinforcement (CAC/A-NW), and with alkaline-treated and further soybean oil-treated reinforcement (CAC/AO-NW). For their production, 4 layers of the correspondent nonwoven fabric (cut to 300 × 300 mm^2) were soaked in the matrix CAC paste (w/c ratio = 0.67). Then, the layers were piled alternating the nonwoven direction (machine and cross direction) in a mold specially designed to apply a 3.5 MPa homogeneous pressure, pressure that was kept for 24 h. Then, the composites were cured in a humidity chamber (approximately 95% relative humidity, 20 °C) for 28 days. For further details, the procedure is described in previous papers [3,28].

Two plates (300 mm × 300 mm × 10 mm) were produced for each composite and, from each plate, six specimens (10 mm × 40 mm × 300 mm) were cut. Three specimens were used to perform the mechanical characterization after curing and the other 3 to analyze the durability of the cured composites after performing an accelerated aging process. The methodology for the accelerated aging [29], consisted on subjecting the material to 4 cycles of 4-day immersion in water at 20 °C followed by 3-day drying in an air-circulating oven at 60 °C.

To determine the flexural behavior, four-point bending tests were carried out following the RILEM TFR1 [30] and TFR4 [31] standards, using an Incotecnic press (*Incotecnic Lab-Pre*, Spain) at a cross-head speed of 4 mm/min and with a 3 kN load cell. The major span (L) was 270 mm, and the displacement measurements were carried out using linear variable differential transformers/sensors (LVDTs) with a 0.01 mm resolution and an error of 0.15%. The following parameters were obtained from the flexural-deflection curves of these tests (see Fig. 5a): a) the limit of proportionality (LOP) defined as the stress value when the first crack appeared; b) the modulus of rupture (MOR) which corresponds to the maximum stress at break or 10% displacement; c) the modulus of elasticity (MOE) as the slope of the elastic zone in the stress-strain curve; and d) the specific energy absorbed as the area under

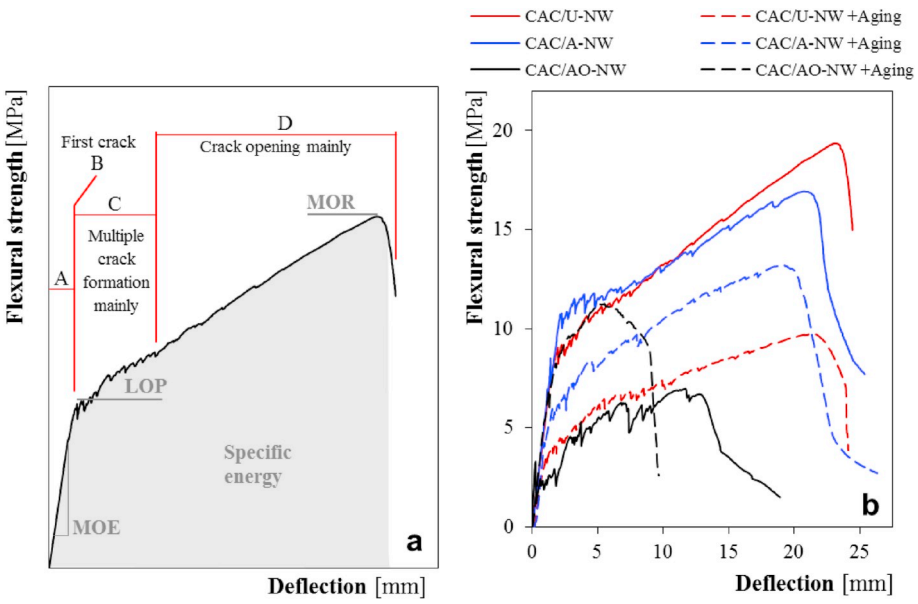

Fig. 5. **(a)** Typical bending curve of the composite material **(b)** Typical bending curves for the composites reinforced with untreated (CAC/U-NW), NaOH treated (CAC/A-NW) and further oil treated (CAC/AO-NW) nonwovens, before and after aging (+Aging).

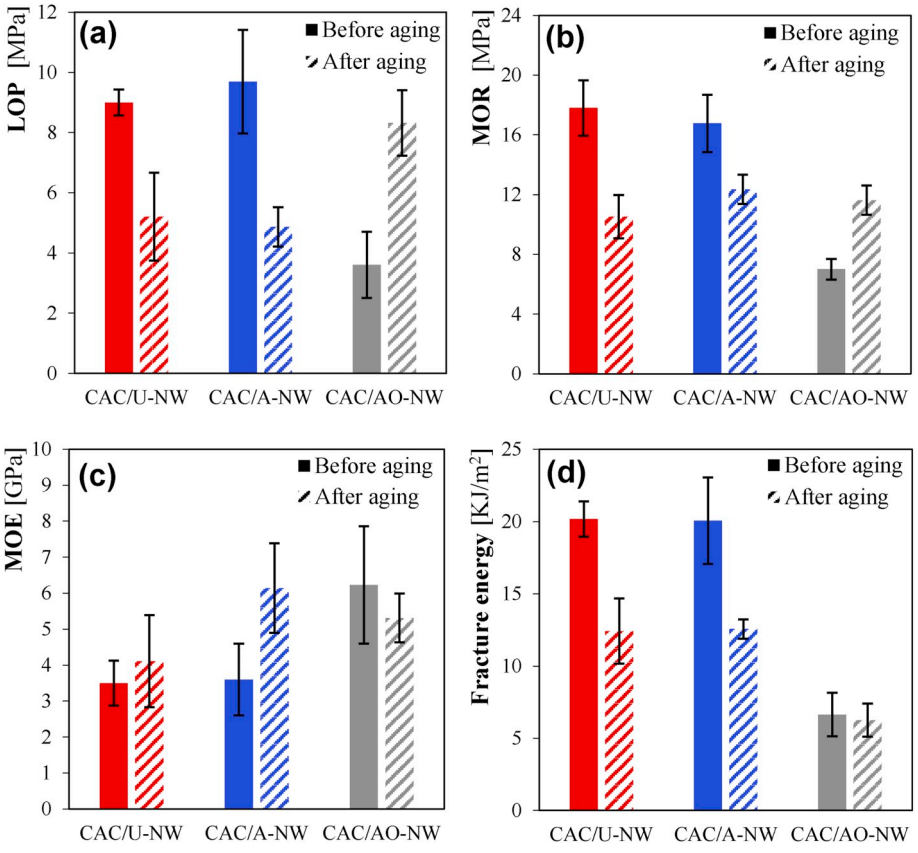

Fig. 6. Comparative four-point bending values of the cement composites reinforced with untreated (CAC/U-NW), NaOH treated (CAC/A-NW) and NaOH and soybean oil treated (CAC/AO-NW) nonwoven, before and after aging: **(a)** LOP, **(b)** MOR, **(c)** MOE and **(d)** fracture energy.

the force-displacement curve (from the starting point of the curve to the value of the ordinate corresponding to a reduction of force equivalent to the 40% of the MOR) divided by the cross-section area of the specimen.

To analyze the cement infiltration through the nonwoven fabrics and the microstructure of the composites, specimens were cut, encapsulated in an epoxy resin and polished, to further obtain backscattered electron microscopy (BSEM) images of the surfaces. Images were taken at 15 kV in a scanning electron microscope (SEM) model JSM-6300 (*Jeol*, Japan), equipped with an energy dispersive X-ray spectrometer (EDS) model Link ISIS-200 (*Oxford Instruments*, United Kingdom) for EDS analysis. An image analysis was performed to determine the hydration degree, which consisted on treating the image to differentiate the pixels by their

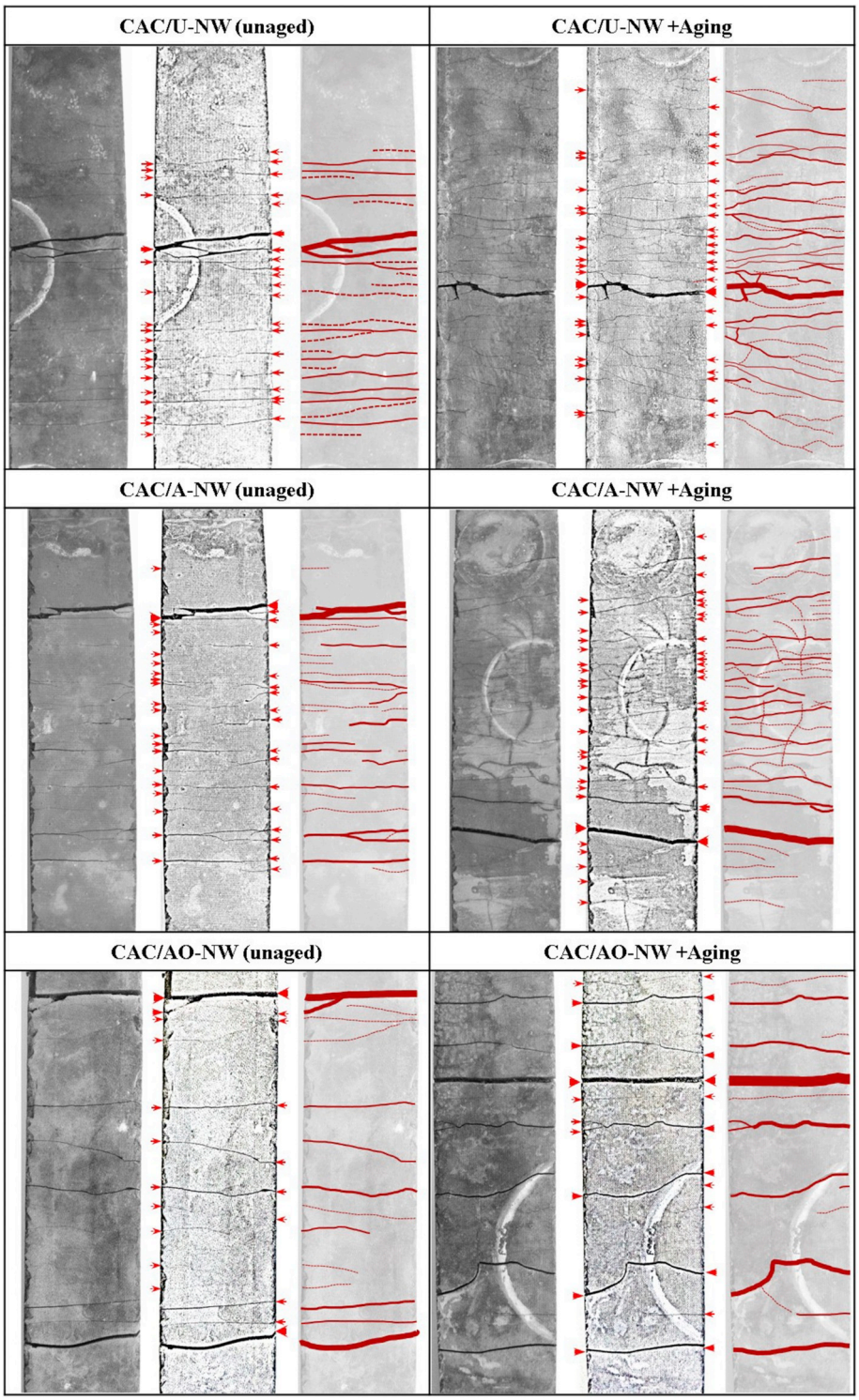

Fig. 7. Crack patterns of the CAC/U-NW composites (top); CAC/A-NW composites (middle) and CAC/AO-NW composites (down) in the unaged (left) and aged (right) states.

different grey intensities corresponding to pores, fibers, and hydrated and anhydride particles as shown in Fig. 2. For each sample, a region of interest (ROI) near the fibers (F-ROI) and far from the fibers, in the matrix (M-ROI) were analyzed to determine differences in the hydration degree.

3. Results and discussion

3.1. Physico-chemical characterization of the nonwovens

The first detergent wash and alkaline treatment (A-NW) of the untreated nonwovens decreased the areal weight from 404 ± 15 to 327 ± 13 g/m^2 or 19.1% loss. As the cellulose content of the nonwoven was 77.1%, nearly 84% of the non-cellulosic components (hemicelluloses,

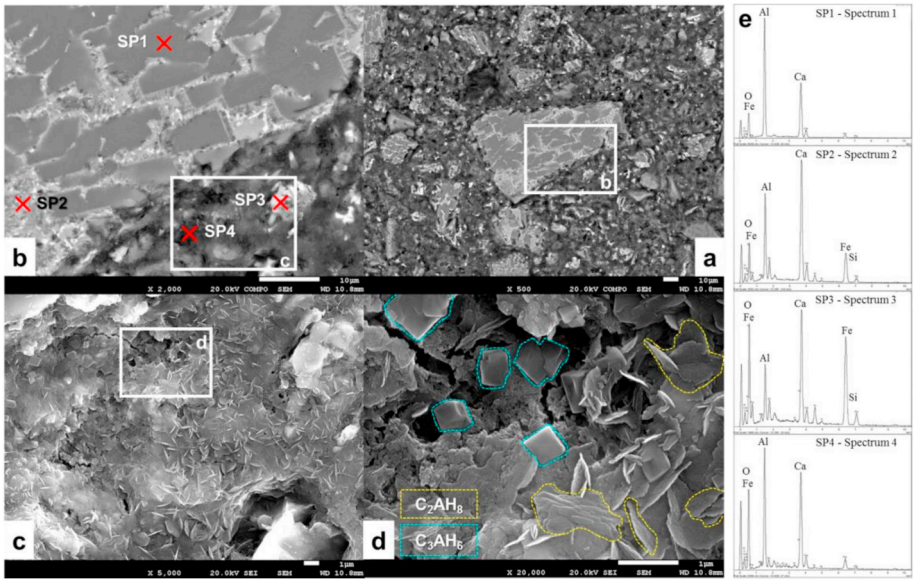

Fig. 8. BSEM images of a CAC cement after 28 curing days with a progressively magnification **(a)** x500, **(b)** x2000, **(c)** x5000, and **(d)** x20000; and EDS spectra **(e)** obtained from areas marked in (b).

lignin and soluble components) were removed by this treatment. The second soybean oil spray treatment deposited around 3.4% by weight.

The substantial removal of the non-cellulosics was confirmed by FTIR (Fig. 3) in which the two spectra for the U-NW and A-NW show the characteristic absorption bands of cellulose at around 3390 cm^{-1}, 2900 cm^{-1}, and 1060 cm^{-1}, which correspond to the stretching vibrations of O–H, C–H and C–O in cellulose, respectively. However, the major spectral differences are found at 2856 cm^{-1}, 1727 cm^{-1} and 1640 cm^{-1}, which are indicative of CH_2 stretching vibration of non-cellulose polysaccharides [32], C═O stretching of acetyl groups of hemicellulose [33] and water absorbance, respectively. Hence, as a consequence of the removal of hemicelluloses, the bands at 2856 cm^{-1} and 1729 cm^{-1} disappeared in the spectra of the treated fibers (A-NW). Moreover, the intensity of the band related to water absorbance diminished on the treated sample.

As expected, for the nonwoven treated with soybean oil (AO-NW), the typical absorption band of carbonyl ester group (1741 cm^{-1}) and the $–CH_2$ stretching symmetric and asymmetric bands at 2856 and 2929 cm^{-1} were observed.

The removal of the non-cellulosic components led to a reduction of moisture absorption from 7.9 ± 0.9% for the U-NW to 5.8 ± 0.1% for the A-NW. The subsequent application of soybean oil (NW-AO) led to a further reduction in moisture absorption to 3.8 ± 0.3%. The water drop absorption time reduced from 47 s for the U-NW to 6 s for the A-NW, showing improved wetting and wicking of the mostly cellulosic nonwoven from the removal of lignin, gums, fatty acids and waxes. The subsequent treatment with soybean oil increased significantly the drop absorption time up to 58 s, proving its effectiveness to achieve a hydrophobic surface.

The NaOH treatment insignificantly increased whereas the subsequent oil treatment significantly reduced the maximum forces to break the nonwovens in machine and cross directions (Fig. 4, level of significance of 5%). During tensile testing, the nonwoven structure elongates with the fibers aligning and the entanglement points stretch up to a maximum force. The increased maximum force values observed on the NaOH treated nonwoven can be attributed to the increased inter-fiber friction from the removal of non-cellulosic components as well as the considerably reduced mass used in normalizing the forces. On the other hand, a decrease of the maximum force was observed on the oil-treated fabrics due to the lubricant effect of the oil, which facilitates fiber sliding and disentanglement.

3.2. Characterization of flax nonwoven-calcium aluminate cement composites

3.2.1. Mechanical performance

Fig. 5a shows the typical bending curve of NW-reinforced cement composites, in which the most relevant zones of the mechanical behavior are marked: (A) matrix behavior, (B) first crack, (C) multiple crack formation —associated to the fiber-matrix adhesion—, and (D) crack opening behavior —associated to the mechanical performance of the reinforcement—. Moreover, the typical bending curves of the nonwoven cement composites are presented in Fig. 5b, from which the values of bending modulus (MOE), limit of proportionality (LOP), modulus of rupture (MOR) and fracture energy were obtained.

Concerning the unaged composites, it can be seen that the bending behavior of the cement reinforced with the untreated nonwovens (CAC/U-NW) and the treated with NaOH (CAC/A-NW) are similar (Fig. 5). Moreover, the zone of the crack generation has a similar profile with multiple peaks, although a greater amount of more pronounced peaks is observed on the composites reinforced with the NaOH treated fabric (CAC/A-NW). This can be related with a higher matrix adhesion in these composites because of the substantial removal of the non-cellulosic components, leading to more homogeneous cellulose surfaces. Moreover, it should be noted that the nonwovens varied in weights depending on the treatment applied, the CAC/U-NW, CAC/A-NW and CAC/AO-NW composites contained different fiber contents of 6.5 ± 0.3 wt%, 5.3 ± 0.2 wt% and 5.6 ± 0.4 wt%, respectively. Hence, despite the fiber weight content in the CAC/A-NW samples is lower than in the CAC/U-NW samples, the crack generation profile points to an even more effective performance of the reinforcement. The last zone, corresponding to the multiple crack formation and crack opening, is almost parallel in both curves. As expected owing to the similar profiles, the main parameters (LOP, MOR, MOE and fracture specific energy) obtained from the curves of this two materials are similar (Fig. 6).

Nonetheless, the composite with soybean oil treated nonwovens had a clearly different bending behavior. The initial linear slope corresponding to the matrix behavior is reduced by 60% with respect to the CAC/U-NW and CAC/A-NW composites. This result indicates that the soybean oil on the fiber surfaces may interact with the cement matrix, possibly modifying its hydration process. In this sense, previous studies [34,35] have reported that the addition of used engine oils in Portland cement and mortars increased the porosity and decrease the flexural

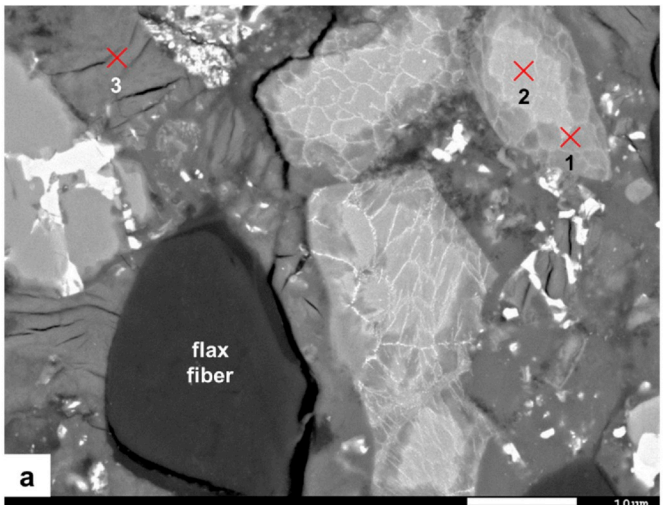

Spectrum	C [%]	O [%]	Mg [%]	Al [%]	Si [%]	Cl [%]	Ca [%]	Ti [%]	Fe [%]
1	9.1	43.3	0.7	9.0	2.5	-	20.4	1.5	13.5
2	10.1	35.8	0.4	18.8	1.9	-	22.2	1.1	9.8
3	10.0	47.1	-	18.8	0.3	0.8	21.9	-	1.2

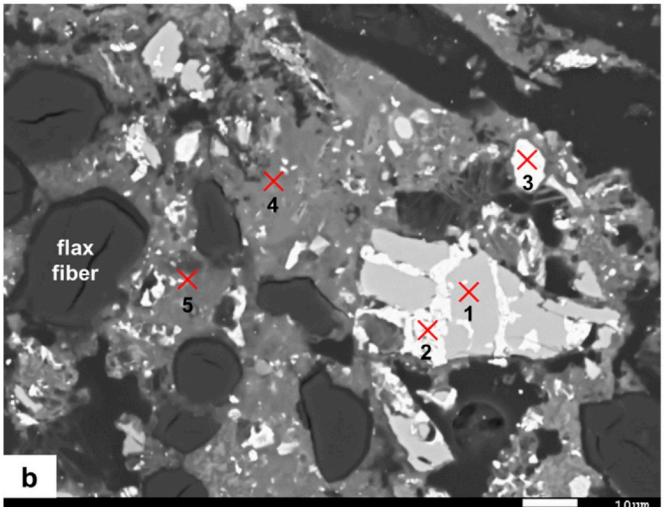

Spectrum	C [%]	O [%]	Mg [%]	Al [%]	Si [%]	Cl [%]	Ca [%]	Ti [%]	Fe [%]
1	10.5	38.2	-	26.9	-	-	20.8	-	3.6
2	14.4	28.9	3.6	6.4	1.6	-	8.5	-	34.6
3	11.6	40.4	0.3	1.2	0.8	-	1.1	2.0	44.7
4	13.2	50.5	-	14.7	1.2	0.4	12.8	-	6.5
5	26.3	44.3	0.4	13.0	0.6	0.4	11.7	0.8	3.5

Fig. 9. BSEM micrographs of the unaged CAC/A-NW **(a)** and the unaged CAC/AO-NW **(b)**, showing the points of the EDS analysis. In (a), the EDS spectra of the analyzed points correspond to: (1) and (2) anhydride CAC particles; and (3) hydrated phases of the CAC. In (b), the spectra correspond to: (1) calcium aluminate; (2) and (3) ferritic phases; (4) and (5) hydrated phases in the cement surrounding the fibers, with higher oxygen content; and (6) flax fiber.

strength. The crack formation zone has a similar profile as those for CAC/U-NW and CAC/A-NW composites, although at a lower flexural strength. Finally, no crack-opening zone is observed in CAC/AO-NW composites. This could be attributed to the overlapping of three different effects: a) decrease of the matrix strength, as observed in the LOP reduction, what would reduce the mechanical performance in the transition zone; b) lower fiber-matrix adhesion owing to the fiber hydrophobicity, achieved as a consequence of the oil treatment; and c) the lower inter-fiber friction due to the oil treatment, that leads to an easier disentanglement of the nonwoven.

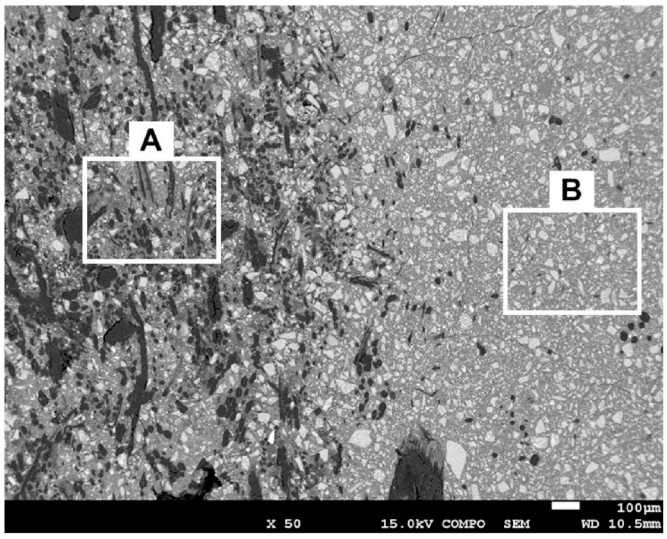

Fig. 10. BSEM micrographs of the unaged sample revealing hydration differences between the matrix near the fibers (left frame, A) and the matrix far from the fibers (right frame, B).

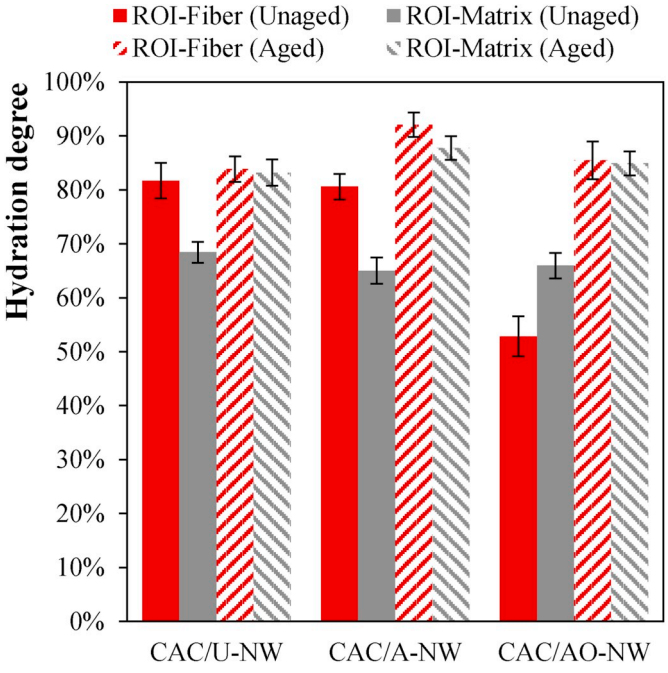

Fig. 11. Hydration degree of the different samples according to the area analyzed (ROI-fiber or ROI-matrix) before and after the accelerated aging.

Upon aging, the bending curves of the CAC/U-NW and CAC/A-NW composites showed similar pre- and post-cracking behavior as their unaged composites while maintaining the strain hardening behavior due to the reinforcement capacity of the nonwovens, but slightly decreased mechanical parameters. The 50% decrease of the LOP value is attributed to the CAC phase change from CAH_{10} to C_3AH_6+$2AH_3$, which leads to higher porosity that has been associated with decreases in both compression and flexural strengths [36–38]. Concerning the crack formation zones, the MOR of both aged samples decreased with that being more significant for the composite reinforced with the untreated (CAC/U-NW + Aging). For the CAC/A-NW, sample, the slope of the crack opening zone (D) of both aged and unaged specimens —which is controlled by the reinforcement behavior— is equal, what points to an

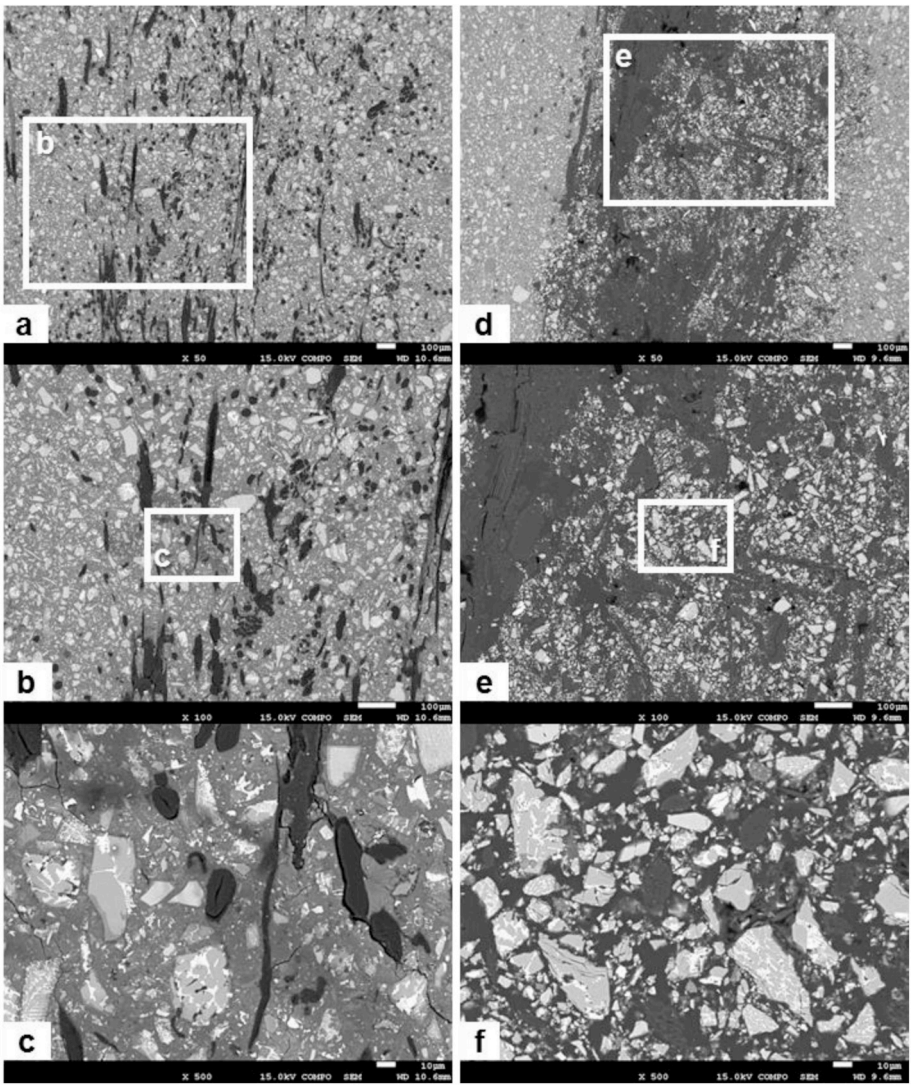

Fig. 12. BSEM images of the ROI-fiber area of the samples: **(a–c)** CAC/U-NW sample, with a regular or even intensive hydration in the area near the fibers; **(d–f)** CAC/AO-NW sample, with an inhibited hydration probably owing to the soybean oil treatment applied to the fibers.

identical behavior of the reinforcing structure. Therefore, the fibers retained their mechanical performance. On the contrary, for the sample CAC/U-NW, the slope of the aged specimen is lower, this pointing to a loss of the fibers' stiffness due to the degradation caused by the matrix.

However, the composite prepared with the soybean oil treated nonwoven (CAC/AO-NW) shown an increase of the LOP value after aging, pointing to a higher strength of the matrix, probably owing to an increase of the cement hydration during the aging process. This is in agreement with the aforementioned effect of the oil's retarding the cement hydration process that continues after curing and during the wet/dry aging cycles. With respect to MOR values, that for aged CAC/AO-NW was similar to those for the CAC/U-NW and CAC/A-NW composites after aging, but was reached at a significantly lower displacement of 6 mm instead of over 20 mm, in part due to its lower LOP due to hydration inhibition of the matrix in presence of oil. Although the soybean oil can be protecting the fibers—keeping their initial stiffness and strength—the decrease of the deflection in crack opening zone from 20 mm to 6 mm points to a higher loss on the fiber-matrix adhesion for the CAC/AO-NW composites.

More insight into the fiber-matrix adhesion may be revealed by examining the fracture energy values (Fig. 6d) and the crack patterns of the samples (Fig. 7). Fiber-matrix adhesion depends on chemical, mechanical and frictional factors. Good chemical affinity has been associated with bending behavior shows multiple crack formation with thinner and less spaced cracks [39,40]. For instance, the fracture energies and the crack patterns for the CAC/U-NW and CAC/A-NW samples before aging are similar, like their mechanical behavior. The pattern with more and thinner cracks of the CAC/U-NW sample (Fig. 7) is consistent with its bending curve in Fig. 5, which shows less pronounced peaks at the crack formation area.

However, a drop of the chemical affinity while the other two factors keep constant is translated into deeper and more spaced cracks in the crack pattern. Since deeper crack leads to a higher stress loss, the bending curves reveal more pronounced and separated peaks in this case. An example is the CAC/AO-NW unaged sample, in which the lower strength of the matrix and the lower fiber adhesion is translated into a pattern with only few wider and more spaced cracks, as revealed by its bending curve. Nevertheless, at a given strain value, the sum of all the crack widths should be equal in all cases. Fiber-matrix adhesion—regardless of the factors involved on it—will lead to high specific energy values owing to the performance of the reinforcement. Only when all three adhesion factors are lost, the specimen will break [39,40].

The trend observed in the aged samples is similar to the one observed in the unaged ones. The CAC/U-NW + Aging and CAC/A-NW + Aging samples present a crack pattern with more, closer and thinner fissures,

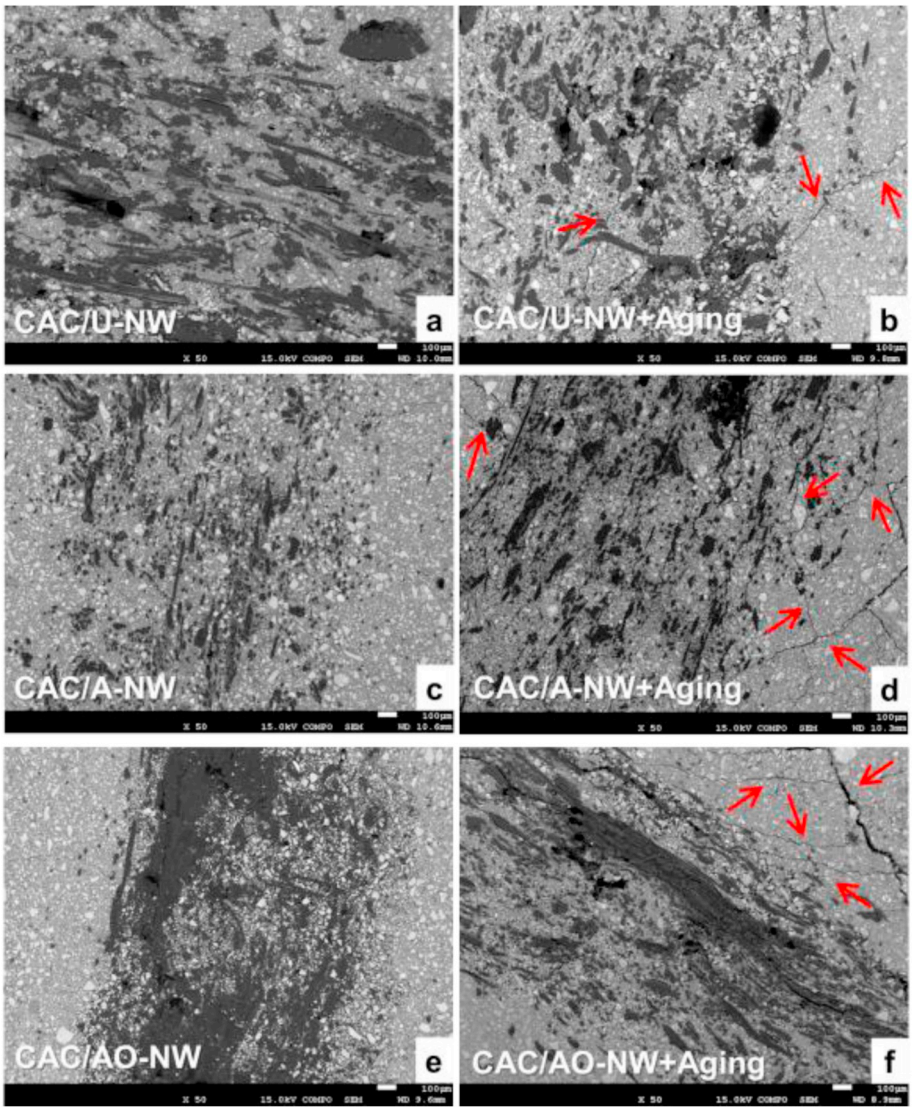

Fig. 13. BSEM micrographs of the unaged composites (left) and of their aged counterparts (right). Images **(a, c, e)** show the cement penetration through the nonwoven. In images (**b, d, f)** the appearance of cracks due to the aging (marked with yellow arrows) can be observed. (For interpretation of the references to colour in this figure legend, the reader is referred to the Web version of this article.)

pointing to a good chemical adhesion and hence, to the effectiveness of the reinforcements. On the other hand, the wider and more spaced cracks of the CAC/AO-NW + Aging sample are consistent with worse mechanical results discussed previously.

3.2.2. *Microstructure*

Fig. 8 presents a progressive magnification of a CAC unreinforced matrix after 28 days curing. In the micrographs, is possible to observe (a) several anhydride polyphasic particles in a more hydrated —darker— and porous phase. The anhydride grains are composed of several phases, which correspond to the different grey tones, as observed in Fig. 8b and their spectra analysis (SP1 and SP2 in Fig. 8e). Most abundant phases are: monocalcium aluminate (CA) found in SP1, and ferritic phases (CA-F, CAS-F) found in SP2 and SP3. Fig. 8c shows a magnification of the hydrated area surrounding the polyphasic particles, revealing an AH_3 amorphous phase — with low porosity—, and also a large amount of laminar-shaped crystals of C_2AH_8 phase (examples marked in green in Fig. 8d). Moreover, on the magnification of the porous area in Fig. 8d, it is possible to observe cubic crystals of the C_3AH_6 stable phase (examples marked in blue), with presence of pores and cracks caused by the volume decrease of the conversion of metastable phases into stable ones. Thus, Fig. 8 reveals that, after 28 days curing, the matrix is at an uncompleted-conversion stage where C_2AH_8 and C_3AH_6 phases coexist.

The composite samples were analyzed in the same way, and it could be observed that the microstructure (Fig. 9) is also formed by polyphasic anhydride grains—with ferritic phases and monocalcium aluminate—and hydrated areas—containing C_2AH_8, identifiable by its laminar shape (Fig. 9a, mark 3) and the stable C_3AH_6 phase in the more porous area—.

The most relevant observation about the composites' microstructure was the heterogeneous distribution of the hydrated phases, since the fibers seemed to affect the paste hydration (Fig. 10).

Hence, an analysis of the hydration degree was performed. Fig. 11 presents the percentage of hydrated compounds in the matrix obtained in fiber-rich areas (ROI-fiber) and areas lacking fibers (ROI-matrix) before and after aging. As can be observed, in the unaged state, the hydration degree in the ROI-matrix areas is similar (around 65–68%) in all the samples regardless the treatment of the nonwoven reinforcement. However, the cement paste found higher water availability in the surroundings of the fibers (ROI-fibers) of the untreated (U) and the alkali treated (A) reinforcements, allowing a better hydration (around 81–82%), while the AO treated reinforcements led to a clearly lower

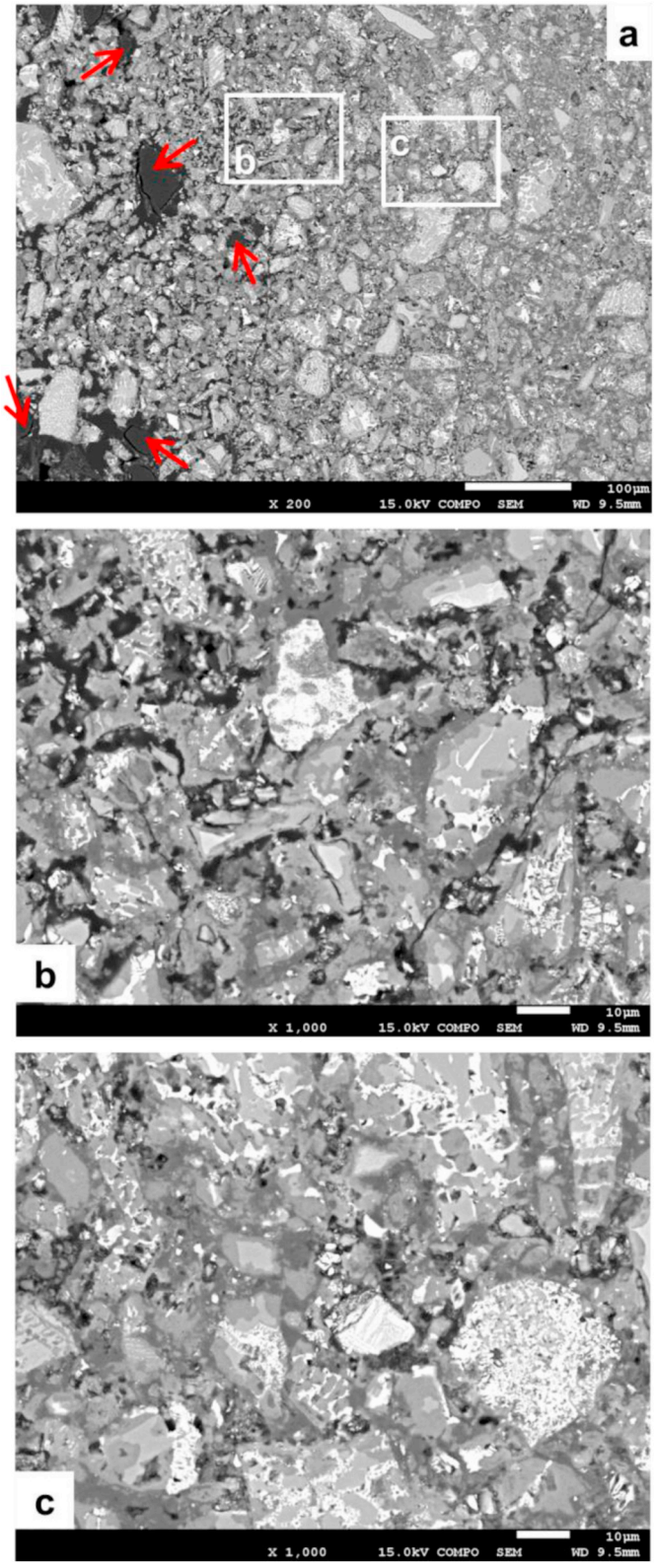

Fig. 14. (a) BSEM micrograph of the aged composite produced with the untreated nonwoven, were the fibers are marked with arrows. The matrix near these fibers **(b)** presents higher porosity and degradation signs than the matrix far from them **(c)**.

hydration degree of 53%. This means that the water availability depends on the water affinity of the fibers, which was affected by the different treatments—higher for the untreated and the alkaline-treated nonwovens and lower for the AO-treated sample. Nevertheless, the wet cycles during accelerated aging level all these differences, allowing water to diffuse throughout the matrix to hydrate all the particles.

Besides, the nonwoven acts as a filter for the bigger cement particles, hence the smaller particles that are capable to penetrate in the nonwoven can be hydrated more easily. As a result, the cement paste in between the fibers in the nonwovens reached a higher hydration—darker grey tone in the SEM images (Fig. 12). Otherwise, the anhydride particles appear sharper and in a larger number in the ROI-matrix area.

In Fig. 13, the BSEM images showing the penetration of the cement in the samples are presented. As can be observed, the penetration is good for the CAC/A-NW composites (Fig. 13c), while the CAC/U-NW and especially the CAC/AO-NW composites achieved a lower penetration, which leads to holes and certain fiber agglomeration (Fig. 13a and e). These fiber agglomerations and voids are also confirmed by the BSEM images of the aged counterparts (Fig. 13b and f).

Otherwise, the aged samples present cracks (Fig. 13b, d and f, marked with arrows), as expected due to the aging process. The cracks located further away from the fibers are deeper and wider and do not seem to advance easily through the nonwoven reinforcement (in the thickness direction), pointing to the effectiveness of the fabric in limiting the crack development.

On the other hand, the SEM images of the CAC/AO-NW sample revealed a large presence of the resin used for sample preparation, especially in the areas near the fibers and even embedding anhydride particles (Figs. 12f and 13e). This last points to a retardation on the matrix hydration, possibly due to the oil presence, as aforementioned. The matrix far from the fibers did not revealed such an effect. The high porosity and low fiber-matrix adhesion reached—as shown by the resin—are in concordance with the poor mechanical properties observed. However, the aging process led to the complete hydration of the particles—once overcome the inhibition effect of the soybean oil—and hence in the CAC/AO-NW + Aging sample only a minor amount of resin could be observed (Fig. 13f).

After accelerated aging, i.e., in the presence of high temperature and humidity, pores were observed in the matrix surrounding fibers in the CAC/U-NW + Aging and CAC/A-NW + Aging samples, signs of degradation. This could be pointing to the fibers that, due to their water retention capability, keep the surrounding area hydrated, enhancing the phase transformation. Since the change from CAH_{10} to C_3AH_6+$2AH_3$ is known to produce a volume reduction [37,38,41], the matrix presents higher porosity in this areas. As shown in Fig. 14, this is clearly observed in the areas near the reinforcement (Fig. 14b), although less intense in the areas far from it (Fig. 14c).

This transformation is consistent with the LOP and MOR decrease observed in these samples. However, the CAC/AO-NW + Aging sample recovered part of the hydration between the fibers, leading to an increase in the mechanical performance of the material, reaching a LOP similar to the samples without aging. Nonetheless, the lower penetration of the paste through the NW, and hence the lack of fiber-matrix adhesion, affected negatively to the specific energy absorbed by the composite.

4. Conclusions

- The NaOH treatment of the fibers reduced their moisture absorption and increased the tensile strength of the nonwovens. Further treatment with soybean oil led to a hydrophobic reinforcement with an even lower moisture absorption.
- The hydrophobization of the nonwovens with the soybean oil led to a reduction of the fiber-matrix interaction, resulting in composites with lower mechanical performance before aging but able to

maintain these properties after accelerated aging. Moreover, the presence of soybean oil in the reinforcement produced an initial inhibition of the hydration, altering the curing of the matrix. Further aging produced a post-hydration of the anhydride particles: the low fracture energy was not further reduced and the LOP and MOR increased significantly.

- The cement composites produced with the NaOH-treated nonwoven presented better mechanical properties than those with the untreated reinforcement even after the accelerated aging, pointing to the effectiveness of the strategy for enhancing fiber-matrix adhesion and decreasing the water absorption.

The findings of this study show that the mechanical performance of flax nonwoven CAC composites is governed more by the fiber-CAC matrix affinity than fiber degradation. Therefore, the NaOH treatment of the flax nonwovens is a good strategy for the production of CAC-based cement matrix composites.

Declaration of competing interest

The authors declare that they have no known competing financial interests or personal relationships that could have appeared to influence the work reported in this paper.

CRediT authorship contribution statement

Laura Gonzalez-Lopez: Investigation, Writing - original draft. **Josep Claramunt:** Conceptualization, Methodology, Resources, Writing - original draft. **You-Lo Hsieh:** Conceptualization, Writing - review & editing. **Heura Ventura:** Supervision, Writing - original draft. **Mònica Ardanuy:** Conceptualization, Methodology, Resources, Writing - review & editing, Supervision.

Acknowledgements

This work was supported by the Ministerio de Economía, Industria y Competitividad [grant number BIA2014-59399-R]. The author Heura Ventura is a Serra Húnter Fellow.

Appendix A. Supplementary data

Supplementary data to this article can be found online at https://doi.org/10.1016/j.compositesb.2020.107955.

References

[1] Yan L, Kasal B, Huang L. A review of recent research on the use of cellulosic fibres, their fibre fabric reinforced cementitious, geo-polymer and polymer composites in civil engineering. Compos B Eng 2016;92:94–132. https://doi.org/10.1016/j.compositesb.2016.02.002.

[2] Ardanuy M, Claramunt J, Toledo Filho RD. Cellulosic fiber reinforced cement-based composites: a review of recent research. Construct Build Mater 2015;79:115–28. https://doi.org/10.1016/j.conbuildmat.2015.01.035.

[3] Claramunt J, Fernández-Carrasco LJ, Ventura H, Ardanuy M. Natural fiber nonwoven reinforced cement composites as sustainable materials for building envelopes. Construct Build Mater 2016;115:230–9. https://doi.org/10.1016/j.conbuildmat.2016.04.044.

[4] Codispoti R, Oliveira DV, Olivito RS, Lourenço PB, Fangueiro R. Mechanical performance of natural fiber-reinforced composites for the strengthening of masonry. Compos B Eng 2015;77:74–83. https://doi.org/10.1016/j.compositesb.2015.03.021.

[5] Olivito RS, Cevallos OA, Carrozzini A. Development of durable cementitious composites using sisal and flax fabrics for reinforcement of masonry structures. Mater Des 2014;57:258–68. https://doi.org/10.1016/j.matdes.2013.11.023.

[6] Fidelis MEA, de Andrade Silva F, Toledo Filho RD. The influence of fiber treatment on the mechanical behavior of jute textile reinforced concrete. Key Eng Mater 2014;600:469–74. https://doi.org/10.4028/www.scientific.net/KEM.600.469.

[7] Barros JAO, Silva F de A, Toledo Filho RD. Experimental and numerical research on the potentialities of layered reinforcement configuration of continuous sisal fibers for thin mortar panels. Construct Build Mater 2016;102:792–801. https://doi.org/10.1016/j.conbuildmat.2015.11.018.

[8] Toledo Filho RD, Silva FDA, Fairbairn EMR, Filho J de AM. Durability of compression molded sisal fiber reinforced mortar laminates. Construct Build Mater 2009;23:2409–20. https://doi.org/10.1016/j.conbuildmat.2008.10.012.

[9] Morton JH, Cooke T, Akers SAS. Performance of slash pine fibers in fiber cement products. Construct Build Mater 2010;24:165–70. https://doi.org/10.1016/j.conbuildmat.2007.08.015.

[10] Arsène M-A, Okwo A, Bilba K, Soboyejo ABO, Soboyejo WO. Chemically and thermally treated vegetable fibers for reinforcement of cement-based composites. Mater Manuf Process 2007;22:214–27. https://doi.org/10.1080/10426910601063386.

[11] Denzin Tonoli GH, De Souza Almeida AEF, Pereira-Da-Silva MA, Bassa A, Oyakawa D, Savastano H. Surface properties of eucalyptus pulp fibres as reinforcement of cement-based composites. Holzforschung 2010;64:595–601. https://doi.org/10.1515/HF.2010.073.

[12] Savastano H, Warden PG, Coutts RSPP. Brazilian waste fibres as reinforcement for cement-based composites. Cement Concr Compos 2000;22:379–84. https://doi.org/10.1016/S0958-9465(00)00034-2.

[13] Dankovich TA, Hsieh Y Lo. Surface modification of cellulose with plant triglycerides for hydrophobicity. Cellulose 2007;14:469–80. https://doi.org/10.1007/s10570-007-9132-1.

[14] Loon LR, Glaus M a. Review of the kinetics of alkaline degradation of cellulose in view of its relevance for safety assessment of radioactive waste repositories. J Environ Polym Degrad 1997;5:97–109. https://doi.org/10.1007/BF02763593.

[15] Van Loon LR, Glaus M a, Laube a, Stallone S. Degradation of cellulosic materials under the alkaline conditions of a cementitious repository for low- and intermediate-level radioactive waste. II. Degradation kinetics. J Polym Environ 1999;7:41–51. https://doi.org/10.1023/a:1021894102937.

[16] De Gutiérrez RMM, Díaz LNN, Delvasto S. Effect of pozzolans on the performance of fiber-reinforced mortars. Cement Concr Compos 2005;27:593–8. https://doi.org/10.1016/j.cemconcomp.2004.09.010.

[17] Toledo Filho RD, Ghavami K, England GL, Scrivener K. Development of vegetable fibre–mortar composites of improved durability. Cement Concr Compos 2003;25:185–96. https://doi.org/10.1016/S0958-9465(02)00018-5.

[18] Santos SF, Schmidt R, Almeida AEFS, Tonoli GHD, Savastano H. Supercritical carbonation treatment on extruded fibre–cement reinforced with vegetable fibres. Cement Concr Compos 2015;56:84–94. https://doi.org/10.1016/j.cemconcomp.2014.11.007.

[19] Almeida AEF de S, Tonoli GHD, Santos SF dos, Savastano Junior H. Carbonatação acelerada efetuada nas primeiras idades em compósitos cimentícios reforçados com polpas celulósicas. Ambient Construído 2010;10:233–46. https://doi.org/10.1590/S1678-86212010000400016.

[20] Tonoli GHD, Santos SF, Joaquim a P, Savastano H. Effect of accelerated carbonation on cementitious roofing tiles reinforced with lignocellulosic fibre. Construct Build Mater 2010;24:193–201. https://doi.org/10.1016/j.conbuildmat.2007.11.018.

[21] Almeida AEFS, Tonoli GHD, Santos SF, Savastano H. Improved durability of vegetable fiber reinforced cement composite subject to accelerated carbonation at early age. Cement Concr Compos 2013;42:49–58. https://doi.org/10.1016/j.cemconcomp.2013.05.001.

[22] Stancu C, Angelescu N, Bratu V. The hydration of super aluminous cement and the mechanical strength development. Sci Bull Valahia Univ – Mater Mech 2012;33–8.

[23] Scrivener KL, Capmas A. 13 - calcium aluminate cements BT - lea's chemistry of cement and concrete. fourth ed. Glob. Prod. Data; 2003. p. 713–82.

[24] Scrivener KL, Cabiron JL, Letourneux R. High-performance concretes from calcium aluminate cements. Cement Concr Res 1999;29:1215–23. https://doi.org/10.1016/S0008-8846(99)00103-9.

[25] Ventura H, Ardanuy M, Capdevila X, Cano F, Tornero JAJA. Effects of needling parameters on some structural and physico-mechanical properties of needle-punched nonwovens. J Text Inst 2014;105:1–11. https://doi.org/10.1080/00405000.2013.874628.

[26] Sasaki K, Tenjimbayashi M, Manabe K, Shiratori S. Asymmetric superhydrophobic/superhydrophilic cotton fabrics designed by spraying polymer and nanoparticles. ACS Appl Mater Interfaces 2016;8:651–9. https://doi.org/10.1021/acsami.5b09782.

[27] Zeng Q, Ding C, Li Q, Yuan W, Peng Y, Hu J, et al. Rapid fabrication of robust, washable, self-healing superhydrophobic fabrics with non-iridescent structural color by facile spray coating. RSC Adv 2017;7:8443–52. https://doi.org/10.1039/C6RA26526J.

[28] Claramunt J, Ventura H, Fernández-Carrasco LJL, Ardanuy M. Tensile and flexural properties of cement composites reinforced with flax nonwoven fabrics. Materials 2017;10:215. https://doi.org/10.3390/ma10020215.

[29] Claramunt J, Ardanuy M, García-Hortal JA, Filho RDT. The hornification of vegetable fibers to improve the durability of cement mortar composites. Cement Concr Compos 2011;33:586–95. https://doi.org/10.1016/j.cemconcomp.2011.03.003.

[30] TFR1- Test for the determination of modulus of rupture and limit of proportionality of thin libre reinforced cement sections, Mater Struct, Vol. 17, No. 102, November-December 1984. n.d.

[31] TFR4- the determination of energy absorption in flexure of thin libre :reinforced cement sections, Mater Struct, Vol. 17, No. 102, November-December 1984 n.d.

[32] Sepperumal U, Selvanayagam S, Markandan M. Characterisation of cellulose produced by Pseudomonas sp. and Actinomycetes sp. Eur J Zool Res 2014;3:13–8.

[33] Cao Y, Chan F, Chui YH, Xiao H. Characterization of flax fibres modified by alkaline, enzyme, and steam-heat treatments. BioResources 2012;7:4109–21. https://doi.org/10.15376/biores.7.3.4109-4121.

[34] Hamad BS, Rteil AA, El-Fadel M. Effect of used engine oil on properties of fresh and hardened concrete. Construct Build Mater 2003;17:311–8. https://doi.org/10.1016/S0950-0618(03)00002-3.
[35] Diab H. Effect of mineral oil on reinforced concrete structures Part I. Deterioration of compressive strength. J Eng Sci Assiut Univ 2011;39:1321–33.
[36] Adams MP. Factors influencing conversion and volume stability in calcium aluminate cement systems. Oregon State University; 2015.
[37] Scrivener KL, Capmas A. Calcium aluminate cements 2001. fourth ed. Elsevier Ltd.; 2001. https://doi.org/10.1016/B978-0-7506-6256-7.50025-4.
[38] Famy C, Scrivener KL, Atkinson a, Brough aR. Effects of an early or a late heat treatment on the microstructure and composition of inner C-S-H products of Portland cement mortars. Cement Concr Res 2002;32:269–78. https://doi.org/10.1016/S0008-8846(01)00670-6.
[39] Cevallos OA, Olivito RS. Effects of fabric parameters on the tensile behaviour of sustainable cementitious composites. Compos B Eng 2014;69:256–66. https://doi.org/10.1016/j.compositesb.2014.10.004.
[40] Fischer G. Fiber-reinforced cement composites by their tensile stress-strain behavior and quantification of crack formation. In: 6th RILEM symp. Fiber-reinforced concr. - BEFIB 2004, Varenna, Italy; 2004. p. 331–8.
[41] Bushnell-Watson SM, Sharp JH. On the cause of the anomalous setting behaviour with respect to temperature of calcium aluminate cements. Cement Concr Res 1990;20:677–86. https://doi.org/10.1016/0008-8846(90)90002-F.